RSC Advances

ROYAL SOCIETY OF CHEMISTRY

www.rsc.org/advances

Journal Name

ARTICLE

Solid transformation synthesis of zeolite from fly ash

Min Xiao[b], Xiaojun Hu[a,*], Yan Gong[b], Dan Gao[b], Peng Zhang[b], Qixin Liu[b], Yue Liu[b] and Muchi Wang[b]

Received 24th August 2015,
Accepted 00th January 20xx

DOI: 10.1039/x0xx00000x

www.rsc.org/

The solid transformation method was carried out to synthesize zeolite from fly ash (FA). The effects of calcination temperature, alkali-fly ash ratio, liquid-solid ratio and crystallization reaction time on the formation of NaA type zeolite and changes of mineralogy were investigated during the synthesis process. The crystal transformation, specific surface area and pore size, and textural properties of zeolite products were characterized by XRD, BET, SEM and TG. The experiment results indicated that zeolite with three kinds of crystal morphology (NaA, SOD, and Ph zeolite) and the higher cation-exchange capacity (CEC) was obtained from coal fly ash in the stage of calcination temperature 650 °C, crystallization temperature 90 °C and crystallization time 3.5 h, liquid-solid ratio 2.7:1 and alkali-fly ash ratio of 0.5:1. The CEC value and adsorption capabilities for Cr(Ⅵ) of FA - derived synthesized zeollite with solid transformation technology were closely similar to that of the commercial grade NaA zeolite.

Introduction

Fly ash (FA) is formed by combustion of coal in power plants as a by-product collected at the top of burner, and its production reaches approximately 850 million tons per year in the world. 52.6% of the FA is used as a raw material, mainly for cement, concrete and soil amendmentproduction.[2]Butthe problem needed to deal with is that in some area, the transportation cost is much higher than the price of FA, so a substantial amount of FA is still disposed in landfills without any management, take up a lot of land and pose widespread environmental and economic problems for heavy metals and other substances. Consequently, the development of methods for greater utilization and production of high value compounds from FA has been the object of recent research. Therefore, more aggressive efforts should be undertaken to effectively develop high value-added utilization of FA. Due to the chemical and mineralogical compositional of FA similarity to volcanic materials with high SiO_2, Al_2O_3 ($SiO_2$and Al_2O_3 60-80 *wt*. %) and aluminosilicate glass content, it is an ideal precursor for high value added zeolite synthesis.[2] Several researches have been successfully prepared various zeolites from FA (ZFA) by hygrothermal conversion processes, salt-thermal, alkali fusion, low temperature, microwave-assisted synthesis, supercritical hydrothermal synthesis and two-step process method, e. g., NaA, NaX, NaP1 zeolite, faujasite, phillipsite and hydroxysodalite (SOD). [3-13]Since NaA zeolite possesses high CEC and water holding capacity, this material is used as catalysts, adsorbent, membrane and cationexchangers.[8, 14-15]The formation of a particular zeolite strongly depends on the ratio of SiO_2/Al_2O_3 in the original FA, temperature, pressure, alkali-fly ash ratio, liquid-solid ratio and time for hydrothermal reaction.

Nevertheless, some problems can arise in these conversion procedures, mostly of which are based on alkaline hydrothermal crystallization requiring large amount of water as solvent for synthesizing zeolites from fly ash, e. g. alkaline pollution, lower yield and higher costs.[2, 7-10]None Liquid-solid transition occurred in the solid phase system and gel phase was depolymerized a rearranged by OH^-. Zeolite structure was formed with trace water fillers.[16]Recently, solid transformation method of zeolite overcome these deficiencies of hydrothermal or nonaqueous system, which can be considered as a friendly environment method for its no mother liquid exists after the crystallization. ZSM-5, ZSM-35, NaA, NaX, NaY zeolite, mordenaite and SOD had been successfully synthesized with solid transformation method in trace water system and dry power system from fly ash.[17-22]However, relative few data are available on the effect of synthesis conditions of FA zeolite on characterization and adsorption performance in solid transformation system.

The present study synthesizes NaA zeolites from FA using solid transformation method, and investigates the effectiveness of calcination temperature, alkali-fly ash ratio; liquid-solid ratio and crystallization reaction time on the formation of zeolite and its properties was investigated. The synthesis products were characterized by XRD, SEM, EDS, specific surface area, cation exchange capacity (CEC) and effectiveness of FA and in removing Cr(Ⅵ) from aqueous solution of its derived ZFA are analyzed. The focus is to establish the proposed supercritical hydrothermal synthesis

[a] School of Chemical and Environmental Engineering, Shanghai Institute of Technology,201418, Shanghai, China.Tel: +86-21-60877210; E-mail address: hu-xj@mail.tsinghua.edu.cn.
[b] Department of Environmental Engineering, Key Laboratory of Regional Environment and Eco-Remediation (Ministry of Education), Shenyang University, 110044 Shenyang, Liaoning, China.

method as a new zeolitization technique and achieve its optimization.

Experimental

Materials and analytical methods

The fly ash supplied from Shenhai Power and Heat Co. Ltd located at Shenyang, China, was ground and sieved to the particle size of smaller than 300 mesh (mean particle size<0.048 mm) and kept in the desiccator before use. The chemical composion of FA before and after removing iron oxide by acid treatment was determined by X-ray Fluorescene Spectroscopy (XRF: Phillips1410, Holland) is listed in Table 1. $K_2Cr_2O_7$ (analytic level) was purchased from Shenyang Xinxi Reagent Plant, China. Deionized water was used in all solution preparations. Cr(Ⅵ) concentration was determined by diphenylcarbazide colorimetric method at 540 nm (V-560 JASCO MHT-344). The uncertainty of this Cr(Ⅵ) assay was less than 5% over five independent measurements of each sample at a concentration of 50 mg·l^{-1}.

Zeolite synthesis

FA used in all experiments was pretreated by the mean of acid treatment. In this stage, FA was refluxed with 2 mol/l hydrochloric acid solution (8 g of fly ash/200 ml of HCl solution) at 80℃ for 1 h to remove Fe_2O_3, which is known to be undesirable for zeolite synthesis. FA was dried at 105 ℃ for 12 h before the experiments. The amorphous SiO_2 and Al_2O_3 components in FA were used as Si and Al sources for synthesis of zeolites. The conversion of FA to zeolites by solid transformation was carried out as follows. An amount of 50 g FA was fused in a muffle furnace at 550-750℃ for 2 h in air atmosphere, the melted materials was then cooled to room temperature and grinded into power. Then 10 g of calcined FA were mixed with 3-10 g of solid NaOH, 6.18g $NaAlO_2$(to control the molar ratio of SiO_2/Al_2O_3=2.2) and 25-30.5 ml H_2O. The slurry was agitated vigorously by mechanical stirrer for 1.0 h at 25℃ and further sealed in a Teflon-lined autoclave and kept at 90℃ for 3-5 h. After cooling to room temperature, the resulting materials were separated into solid phase and treating solution by filtration. The solid phased was thoroughly washed with distilled deionized water until pH<7, and dried at100 ℃for 24h in an air oven, ground to pass through 300 mesh sieve and stored in the desiccator. The products obtained were labeled as ZFA.

A series of methodologies were tested by using different calcination temperature, alkali-fly ash ratio, liquid-solid ratio and crystallization time, quantity of aluminum, etc. to determine the optimal conditions to the synthesis of the pure NaA zeolites from FA by solid transformation. The quantity of aluminum was strictly controlled (the molar ratio of SiO_2/Al_2O_3=2.2), which was crucial for avoiding the formation of other zeolitic phases when the relevant zeolite is being formed.[16]

Determination of Cation exchange capacity and Specific surface area

The CEC value of FA and NaA ZFA were characterized by the ammonium acetate method, and compared to that of the commercial grade NaA zeolite. Accordingly, the sample was initially saturated with Na^+ and freed from organic impurities after being washed thrice with sodium acetate solution and subsequently with 99% isopropyl alcohol, respectively. Finally, the Na^+ was exchanged with NH_4^+ after washing the sample thrice by ammonium acetate solution, and took the average.

The specific surface areas of zeolite samples were determined by a by fitting the linear portion of the BET plot to BET equation, and pore size distribution was calculated based on the desorption plot of N_2adsorption–desorption isotherm using the Barrett–Joyner–Halenda (BJH) method (Micrometrics ASAP 2000, USA).

Material characterizations

The mineralogical composition of FA and synthesized products zeolite were determined by using X-ray Diffraction Spectroscopy(XRD: Bruker-AVS D8 Advance Powder Diffractometer, USA) with diffraction angle (2θ) ranging from 0 to 80° using Cu Kα radiation at 40kV and 40mA, and the diffractograms are presented in Fig. 1-5. The minerals, present in the sample were identified by matching actual spacing of an unknown mineral with the diffraction data file (JCPDS 43-0142). Accordingly, designations; Q, M, H, A, S and Ph used in Fig. 1-9, represent the minerals Quartz (JCPDS 85-0796), Mullite (JCPDS 74-4143), Hematite (JCPDS 33-0664), zeolite NaA (JCPDS 43-0142), Hydroxysodalite (JCPDS 31-1271) and Philipsite (JCPDS 39-1375), respectively. Surface morphology of FA and synthetic zeolite was analyzed by scanning electronic microscopy (SEM, HITACHI, S-4800, Japan) coupled with energy dispersive X-ray analysis (EDAX). In the SEM analysis, the samples were coated with a thin layer of gold to make them conductive. The synthetic zeolite was further characterized by thermogravimetric analysis (TGA) and differential thermal analysis (DTA) set up (Diamond TG/DTA, PERKIN ELMER, USA) with a heating rate of 10 ℃·min^{-1} from ambient temperature to 800°C in argon atmosphere.

Results and discussion

XRD patterns and CEC values of fly ash and synthesized zeolite by fusion prior to solid transformation method at 60min at different calcination temperature is shown in Fig. 1 and 2.

As shown in Fig. 1, FA is mainly composed of a silica rich glassy phase with minor amounts of mullite and quartz. The X-ray diffractions after crystallization shows the crystalline phase of quartz and mullites were gradually distinguished. The main crystalline phase was identified as NaA zeolite as JCPDs number 43-0142, with small amounts of SOD and Ph zeolites. With the increasing of calcination temperature from 550 ℃to 700 ℃, characteristic peaks of NaA zeolite tend to increase appreciably and then decreased in intensity. As can be seen in Fig. 2, the maximum CEC value occurs at 650℃. This behavior coincides with the mechanism of process for zeolite formation from typical sources of aluminum and silicon.[8, 23]The reduction in peak intensities at 700 ℃ may be the result of the transformation of NaA zeolite to the Ph *and* SOD zeolites, [7]

which have lower cation exchange capability and then the adsorption performance of ZFA decreased.

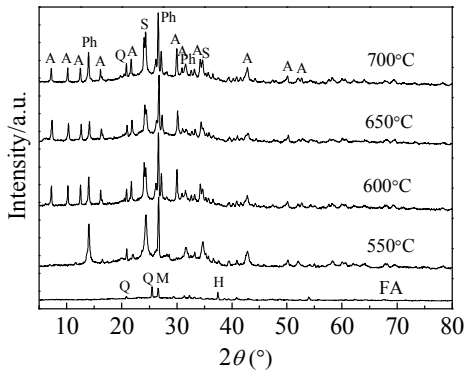

Fig. 1 XRD patterns of original FA and zeolites synthesized by solid transformation at various calcination temperatures with alkali-fly ash ratio 0.5:1 for 60min

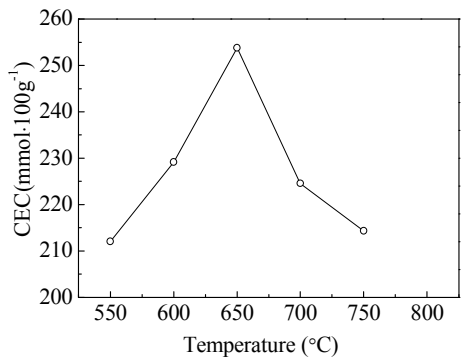

Fig. 2 Effect of calcination temperature on CEC of ZFA

The XRD patterns of the FA zeolites obtained with various alkali-fly ash mass ratios from 0.3 to 0.9 are shown in Fig. 3, and the peak was consistent with the NaA type characteristic peak at 0.5. The effect of alkali-fly ash ratios on CEC of ZFA is presented in Fig. 4 was consistent with the trend, the better adsorption capacity was markedly at 0.5 of alkali-fly ash mass ratios. It is clearly seen that the peak intensities of NaA zeolite increased with the raising of alkali-fly ash ratio and then gradually decreased when it was increased to above 0.9. It is also found the XRD peak intensity of NaA zeolite was much low until the alkali-fly ash ratio was greatly increased to above 0.3. When the ratio was very low (~0.3 $g \cdot g^{-1}$), only part of the glass phase (mainly mullite and quartz) dissolved in supercritical water. The reactions were more active with the increase of the alkali-fly ash ratio to above 0.3. The glass phase thoroughly disappeared and the dissolution of Si and Al accelerated the zeolite formation.[24-26]The results indicated that the high alkali-fly ash ratio leading to the fusion of more mullite and quartz in raw material and the formation of more NaA zeolite. When the alkali-fly ash ratio changed from0.3 to 0.5, the grain size of mullite and quartz decreased with the raising of the alkali-fly ash ratio, while the size of crystals generated was gradually enlarged and the crystal form became more complete. But the excess NaOH will restrain the formation of NaA zeolite and promote that of SOD and Ph zeolite. [27]A dispersion system of FA and trace water was formed in the solid transformation synthesis process, of which aluminosilicate and adsorbed water as adsorbent and the adsorbate, respectively. Solid phase system entropy increased significantly due to the dispersion of NaOH power and generation of surface bond on the surface of aluminosilicate, which led to the formation of electric field gradient, potentiometric gradient and concentration gradient and promoted the self-diffusion of Na^+ and OH^-,[17-19] and aluminosilicate could be depolymerized an rearranged by OH^-.

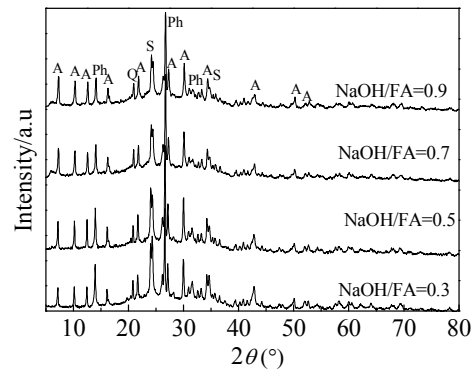

Fig. 3 XRD patterns of zeolite under various alkali-fly ash ratios (Reaction conditions: 650℃, 60min)

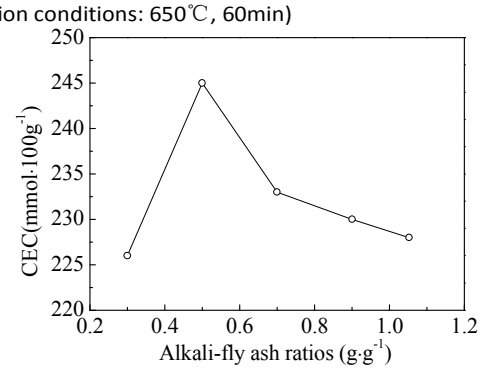

Fig. 4 Effect of alkali-fly ash ratios on CEC of ZFA

The XRD patterns of the FA zeolites obtained from various liquid solid mass ratios are shown in Fig. 5. It can be found that the quartz and mullite phases almost disappeared, and the main crystalline phase of NaA zeolite can be observed at 2.5:1. The effect of liquid solid mass ratios on CEC of ZFA is presented in Fig. 6, with the increasing of liquid solid ratios from 2.4 to 3.0 $g \cdot g^{-1}$, CEC values increased appreciably and then decreases rapidly, the maximum was obtained at 2.7:1 $g \cdot g^{-1}$. The dispersion system of NaOH, FA and trace water could be difficult to form at lower liquid solid ratios, which aluminosilicate and adsorbed water as adsorbent and the adsorbate, and aluminosilicate could not be depolymerized an rearranged by OH^-. The crystal peak intensity of NaA zeolite increased as the liquid–solid ratio increased from 2.4:1 to 2.7:1 and then decreased. Furthermore, it can be seen from Fig. 5, which the XRD intensities of quartz and mullite steadily

decreased when the liquid solid mass ratio is increased from 2.4:1 to 2.88:1. The major crystalline phase was SOD at lower liquid–solid ratio of 2.4:1. The higher liquid–solid ratio could cause the low alkalinity and the transformation of NaA zeoliteto the SODand Ph zeolites accordingly. Therefore, the appropriate liquid–solid volume ratio is 2.7:1.

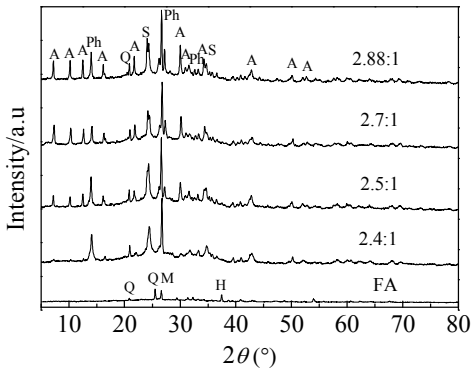

Fig. 5 XRD patterns of zeolite obtained from various liquid-solid ratios (Reaction condition: alkali-fly ash ratio 0.5:1, 90℃, and 3.5h)

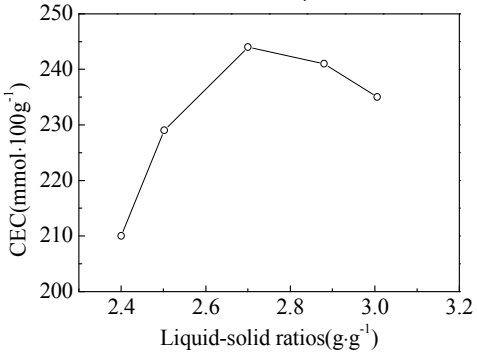

Fig. 6 Effect of liquid-solid ratios on CEC of ZFA

XRD pattern of FA zeolite in different crystalline time at 90℃, alkali-fly ash ratio 0.5:1, liquid-solid ratio: 2.7:1 are shown in Fig. 7. It was showed that NaA zeolites were the main crystalline phases from 3 to 4.5 h, and their XRD intensities increased and that of quarze and mullite decreased with the increase of reaction time. The characteristic peaks of NaA zeolite increased gradually with the reaction time. As can be observed in Fig.8, the adsorption of ZFA increased with the rise of crystalline time and declined rapidly, the preferable adsorption capacity was attained at 3.5 h. NaA zeolite tends to transform into SOD and Ph zeolite upon prolonged reaction time.

Fig. 9 showed X-ray patterns of zeolite synthesized obtained from fly ash. According to the diffractograms, the major crystalline phase was identified as NaA zeolite as JCPDS number 43-0142, with small amounts of SOD and Ph zeolite. Quartz normally found in the diffractograms of fly ash could not be completely dissolved during the hydrothermal treatment and remained in the zeolite product after the synthesis. The original fly ash which presented the high content of aluminum, gave rise to the products of three kinds of zeolite (NaA, SOD, and Ph zeolite). Hydroxysodalite zeolite has high stability under variations of temperature and can occur during the synthesis of zeolites using coal fly ash as raw material crystallized between 353.15 K and 413.15 K. [28] The content of Ph zeolite increased with crystalline time and gradually replaced SOD zeolite. [23, 29]

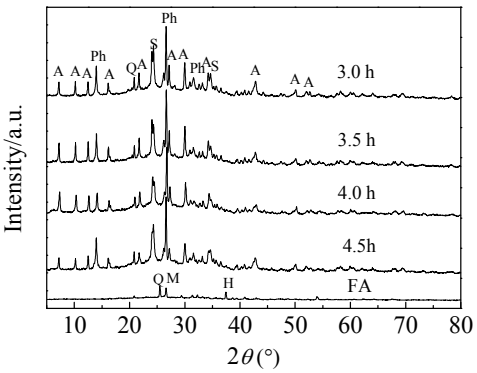

Fig. 7 XRD patterns of zeolite obtained from various crystalline time (Reaction condition: alkali-fly ash ratio 0.5:1, 90 ℃, liquid-solid ratio: 2.7:1)

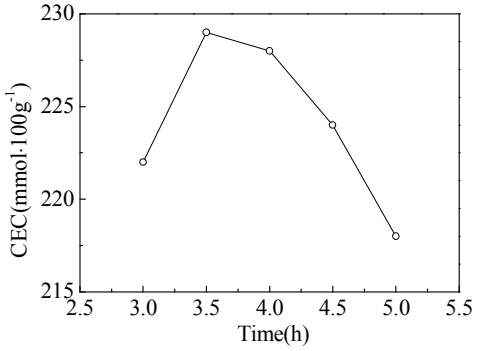

Fig. 8 Effect of crystallization time on CEC of ZFA

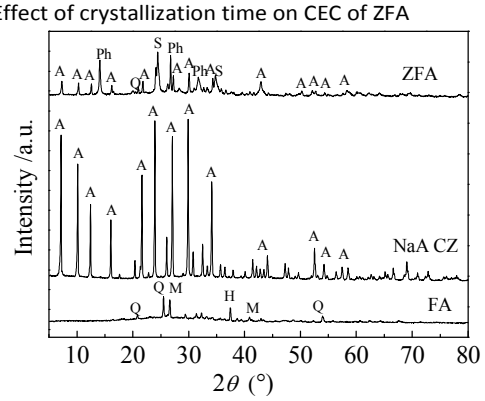

Fig. 9 Comparison of XRD of coal fly ash, synthetic zeolite from fly ash using solid transformation method and NaA commercial zeolites

Moreover, SEM photos indicated the uniform. According to literature, NaA zeolite presents a cubicstructure.[4, 7-10, 30] SEM images of fly ash, synthesized zeolite by solid transformation

method and its EDS analysis can be compared in Fig. 10. The spherical particles with relatively smooth surface and irregular round shaped predominated for the raw FA in Fig. 10(a). The SEM micrographs of Fig. 10(b)-(c) conform the major crystalline phase was NaA zeolite, and the minor crystalline phase was Ph and SOD zeolites with rhombic and octahedral crystal, which consists with the reported literature.[7, 23, 31, 32]

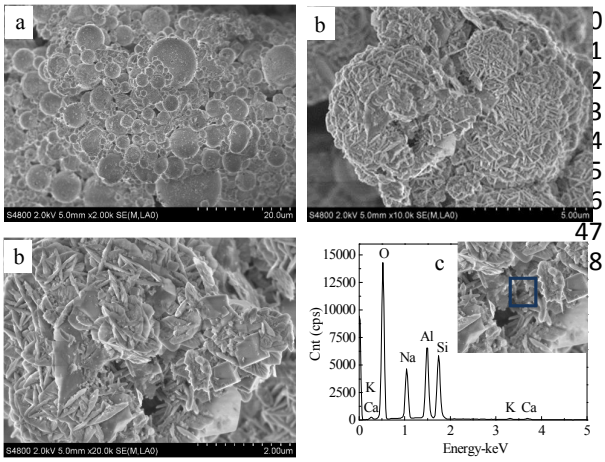

Fig. 10 SEM image of fly ash (a), the synthesized crystalline NaA zeolites from fly ash with solid transformation method (b) and EDS of the synthesized zeolite (c)

Thermal analysis curves (TG and DTA) of the synthesized NaA zeolite is shown in Fig. 7.

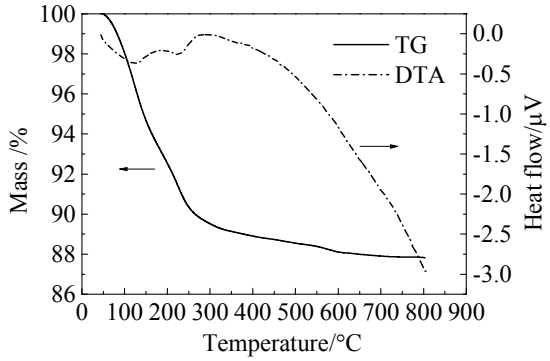

Fig. 11 Thermal analysis (TG, DTA) curves of synthesized NaA zeolite

Endothermic peak exists in the DTA and weight losing slope in the TGA curve demonstrates the maximum rate of H_2O loosing is temperature around 200 ℃. According to the TGA curve, the maximum weight loss, which is corresponded to water content of the sample, is about 12 wt.%. The DTA curve of the as-synthesized zeolite shows several thermal effects. The first endothermic effect with its maximum around 200-250℃ is relevant to water release from NaA zeolite,[9] accompanied by sharp and sudden loss of mass. It seems that an exothermic effect at 500-540 ℃ may be connected with partial decomposition of the NaA zeolite structure. Usually a process of crystal decomposition is of exothermic character. Moreover, in certain cases it has been reported that decomposition of zeolites is related to the collapse of free duct spaces at this temperature.

The chemical composition of ZFA was shown in Table 1. Silica, alumina, iron oxide, sodium oxide and calcium oxide are the mainly chemical composition. A significant amount of Na element is incorporated in the final product due to hydrothermal treatment with solid NaOH. Due to dissolution of SiO_2 by the hydrothermal treatment, the content of this compound in ZFA decreased. The SiO_2/Al_2O_3 mole ratio 2.13 for the ZFA product is close to NaA ($NaAlSiO_{4.2}$-$2.25H_2O$, SiO_2/Al_2O_3 2.0) type zeolite.

Table 1 Chemical composition of fly ash and fly ash after removed iron oxide by mean of XRF technique (*wt*.%)

Components	FA	FA after removed Fe_2O_3	ZFA
SiO_2	34.90	68.9	42.2
Al_2O_3	17.20	20.1	33.6
CaO	26.30	2.85	2.13
MgO	1.87	0.975	0.35
Fe_2O_3	8.28	3.02	2.69
K_2O	1.14	2.85	0.92
Na_2O	0.73	0.60	17.4
Others	7.70	1.49	0.71
SiO_2/Al_2O_3 (mol/mol)	3.45	5.82	2.13

Specific surface area was measured by BET method. Fig. 12 and Table 2 shows the specific surface area, cation exchange capacity (CEC) and total pore volume of the synthesized hybrid (NaA, SOD, and Ph) zeolite are 14.48 m^2/g, 253.86 mmol/100 g and 0.035 cm^3/g, respectively. These values are in accordance with the data found in literature.[4, 19, 23, 27] The adsorption branches of the N_2 sorption isotherms revealed I type of IUPAC classification, indicating the existence of microporous materials. Generally the NaA type zeolite products provided micropore structures with one broad capillary condensation step at p/p_0 of 0.05-0.95, representing the broad pore size distribution of which normally observed with NaA type zeolite.

It clearly shown that the BET surface area, CEC and total pore volume and which exhibited 81.99%, 90.89%, and 70.0% that of commercial NaA zeolite, and higher than that of the raw fly ash. The CEC values presented by the pure NaA type zeolites synthesized from FA with alkaline fusion method are higher than that of hybrid materials produced at current study.[27] While the CEC value of ZFA in our work is much higher than those of products synthesized using one-step hydrothermal treatment.[15]

The characteristic and adsorption capacity of ZFA by solid transformation method was investigated in comparison to that

of FA, commercial zeolite(CZ), NaA ZFAs reported in related references, and the test to remove Cr(Ⅵ) from aqueous solution was conducted at pH 3.12 under the same conditions. According to Fig. 9, the rate of uptake of Cr(Ⅵ) was quite rapid; at equilibrium, the time-dependent amount of Cr(Ⅵ) adsorption were 2.1 mg·g^{-1} for FA, 7.6-8.7 mg·g^{-1} for ZFAs and 8.7 mg·g^{-1} for CZ, respectively, which indicated that the ZFA was much effective than FA, and was similar to CZ, and zeolites synthesized from fly ash was found to successfully remove Cr(Ⅵ) from aqueous solution. The adsorption capacity and CEC value of NaA using alkaline fusion method in our work team was as well as that of NaA commercial zeolite, which was superior to ZFA with solid transformation in this work. It could be due to the SOD and Ph zeolite in this hybrid material.

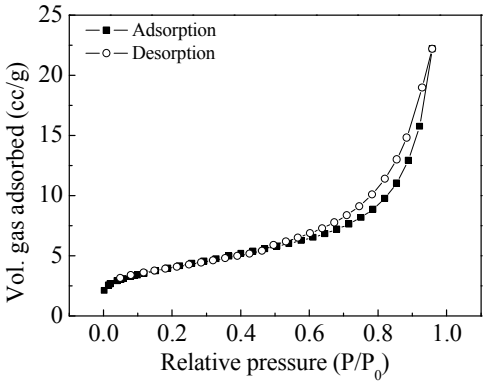

Fig. 12 N_2 sorption isotherms of NaA ZFA

Table 2 Cation exchange capacity (CEC) of the synthesized zeolite NaA in comparison to raw FA and some related NaA zeolites from FA

Sample	SBET ($m^2 \cdot g^{-1}$)	CEC (mmol·100g^{-1})	Total pore volume ($cm^3 \cdot g^{-1}$)	Average pore size (nm)
FA	9.9	15.6	0.016	15.3
CZ	17.66	279.31	0.050	0.30
ZFA[a]	14.48	253.86	0.035	0.49
NaA[b]	16.12	357.31	0.028	0.34
NaA[c]	41.2	400.0		
NaA[c]	36.1	377.0		

[a] ZFA: Synthesized zeolite from fly ash with solid transformation method. This work.
[b] NaA: Synthesized zeolite from fly ash with alkaline fusion method. Our team.
[c] NaA: Synthesized zeolite from fly ash with alkaline fusion method. (Ref. [27])

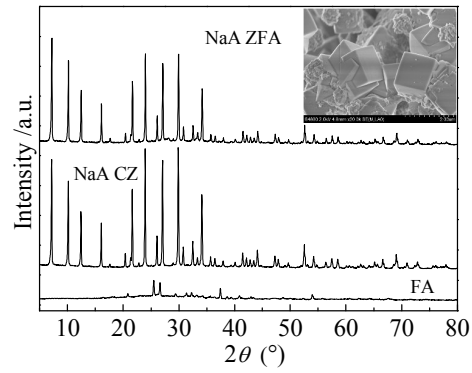

Fig.13 XRD patterns of FA, CZ and NaA ZFA using alkaline fusion method and SEM image of NaA ZFA in our work team

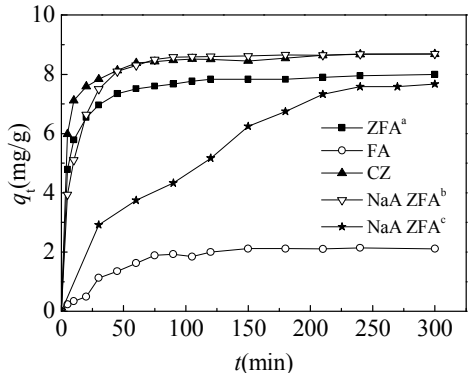

Fig. 14 Efficiency of Cr(Ⅵ) over FA, Commercial NaA zeolite and zeolite synthesized by FA
C_0=50.26 mg·l^{-1}, pH=3.12, dosage=5 g·l^{-1}, T=25℃
([a] ZFA: Synthesized zeolite from fly ash with solid transformation method. This work.
[b] NaA ZFA: Synthesized zeolite from fly ash with alkaline fusion method. Our work team.
[c] NaA ZFA: Synthesized zeolite from fly ash with alkaline fusion method. (Ref. [26])

Conclusions

NaA Zeolite (with small amounts of SOD and Ph zeolite) was converted from FA, by means of solid transformation method in trace water system. Results revealed that the mixture of FA and $NaAlO_2$with the molar ratio of SiO_2/Al_2O_3 of 2.2 can be converted to NaA zeolite at the crystallinity temperature and time of650 °C and 60 min, alkali-fly ash ratio 0.5:1 crystallization temperature and time 90 °C and 3.5h, liquid-solid ratio 2.7:1, it is easy to form NaA zeolite. The synthesized FA zeolites can be well used as sorbents for the removal of Cr(Ⅵ) from aqueous solution. Formation of NaA zeolite was ascertained by mean of different characterization techniques including XRF, XRD, SEM, TGA/DTA, BET. The XRD results revealed that the major crystalline phase was identified as NaA zeolite, with small amounts of SOD and Ph zeolite. The morphology of synthesized product also indicated the cubic structure crystal of NaA, and minor crystalline phase was

rhombic, octahedral and cubic crystal. The results were confirmed by CEC and BET techniques. The CEC and specific surface area of NaA were 253.86 mmol·100g^{-1} and 14.18 m^{2}g^{-1}, respectively.

Acknowledgements

This work was supported by the National Natural Science Foundation of China (21277093), Program for New Century Excellent Talents in University (NCET-13-0910), General Project of Liaoning Provincial Department of Education (L2015361), Liaoning BaiQianWan Talents Program (2014921003), the Science and Technology Program of Shenyang City of China (F13-062-2-00) and the Competitive Selection Project of Shenyang Scientific Undertaking.

References

1 M. Ahmaruzzaman,*Prog.Energ. Combust.*, 2010, 36, 327.
2 S. S. Bukhari, J. Behin, H. Kazemian and S. Rohani, *Fuel*, 2015, 140, 250.
3 H. Holler, U.Wirsching,*Forchr Miner*, 1985, 63, 21.
4 J. C. Izidoro, D. A. Fungaro, J. E. Abbott and S. Wang, *Fuel*, 2013, 103, 827.
5 H. Tanaka and A.Fujii, *Adv.Powder Technol.*, 2009, 20, 473.
6 B. Jha and D. N. Singh, *Appl.Clay.Sci.*, 2014, 90, 122.
7 M. Zhang, H. Zhang, D. Xu,L. Han, D. Niu, L. Zhang, W. Wu and B. Tian, *Desalination*, 2011, 277, 46.
8 J. Wang, D. Li, F. Ju, L. Chang and W. Bao, *Fuel Process.Technol.*, 2015, 96, 136.
9 H. Kazmian, Z. Naghdali, T. G. Kashani and F. Farhadi, *Adv. Powder Technol.,* 2010, 21, 279.
10 W. Franus, *Pol. J. Environ. Stud*., 2012, 21(2), 337.
11 M. Wdowin, M. M. Wiatros-Motyka, R. Panek, L. A. Stevens, W. Franus and C. E. Snape, Fuel, 2014, 128, 451.
12 W. Franus, M. Wdowin, and M. Franus, Environ. Monit. Assess., 2014, 186(9), 5721.
13 L. Bandura, M. Franus, G. Józefaciuk, and W. Franus, Fuel, 2015, 147, 100.
14 C. Belviso, F. Cavalcante, F. J. Huertas, A. Lettino, P. Ragone and S. Fiore, *Micropor.Mesopor.Mat.,* 2012, 162, 115.
15 N. M. Musyoka, L. F. Petrik, E. Hums, H. Baser and W. Schwieger, *Catal.Today,* 2012, 190, 38.
16 A. M. Cardoso, M. B. Horn, L. S. Ferret, C. M. N. Azevedo and M. Pires, *J. Hazard. Mater.*, 2015, 287, 69.
17 Y. Liu, D.Li and X.Wang, *China Surfactant Detergent & Cosmetics.*, 2002, 32, 53.
18 S. Catidge and W. M. Meier, *Zeolites*, 1984, 4, 218.
19 R. Tsai, K. Du, T. Cheng, G. H. Ho, P. Wu, S. Liu and T. Tsai, *Catal. Today*, 2013, 204, 30.
20 C. Ferone, B. Liguori, A. Marocco, O. Omotoso, W. Friesen, C. Fairbridge, Y. Shi and S. Ng, *Micropor. Mesopor. Mat.*, 2010, 134, 65.
21 J. H. Zhang, M. B. Yue, X. N. Wang and D. Qin, *Micropor. Mesopor. Mat.*, 2015, 217, 98.
22 H. Feng, X. Chen, H. Shan and J. W. Schwank, *Catal. Commun.*, 2010, 11, 700.
23 J. C. Izidoro, D. A. Fungaro, F. S. Santos and S. Wang, *Fuel processing technology*, 2012, 97, 38.
24 M. Lee, G. Yi, B. Ahn and F. Roddick,*Korean J. Chem. Eng*, 2000, 17, 325.
25 H. Tanaka, S. Matsumura and R. Hino, *J. Mater. Sci.*, 2004, 39, 1677.
26 S. H. Asl, M. Ahmadi, M. Ghiasvand, A. Tardast and R. Katal. *J. Ind. Eng. Chem.*, 2013, 19, 1044.
27 M. Chareonpanich, O. Jullaphan and C. Tang. *J.Clean.Prod.*, 2011, 19, 58.
28 C. Poole, H. Prijatama and N.M. Rice, *Miner. Eng.*, 2000, 13, 831.
29 Q. Xavier, A Andres, L. Jose, T. Fernandez and L. S. Angel, *Fuel*, 1995, 74 (8), 1226.
30 R. Panek, M. Wdowin and W. Franus, In International Multidisciplinary Microscopy Congress. Springer International Publishing, 2014, 45.
31 G. Atun, G. Hisarh, A. E. Kurtoglu and N. Ayar. *J. Hazard. Mater.,* 2011, 187, 562.
32 N. Koukouzas, C. Vasilatos, G. Itskos, I. Mitsis and A. Moutsatsou, *J. Hazard. Mater*., 2010, 173, 581.
33 S. Chałupnik, W. Franus, M. Wysocka and G. Gzyl, *Environ.l Sci. Pollut. Res.*, 2013, 20(11), 7900.